Wild Band Edges: The Role of Bandgap Grading and Band-Edge Fluctuations in High-Efficiency Chalcogenide Devices

Preprint

Ingrid Repins,[1] Lorelle Mansfield,[1] Ana Kanevce,[1] Søren A. Jensen,[1] Darius Kuciauskas,[1] Stephen Glynn,[1] Teresa Barnes,[1] Wyatt Metzger,[1] James Burst,[1] Chun-Sheng Jiang,[1] Patricia Dippo,[1] Steve Harvey,[1] Glenn Teeter,[1] C. Perkins,[1] Brian Egaas,[1] Andriy Zakutayev,[1] Jan-Hendrik Alsmeier,[2] Thomas Lußky,[2] Lars Korte,[2] Regan G. Wilks,[2] Marcus Bär,[2,3] Yanfa Yan,[4] Stephan Lany,[1] Pawel Zawadzki,[1] Ji-Sang Park,[1] and Suhuai Wei[1,5]

[1] *National Renewable Energy Laboratory*
[2] *Helmholtz-Zentrum Berlin für Materialien und Energie GmbH*
[3] *Brandenburgische Technische Universität Cottbus-Senftenberg*
[4] *University of Toledo*
[5] *Beijing Computational Science Research Center*

Presented at the 43rd IEEE Photovoltaic Specialists Conference
Portland, Oregon
June 5–10, 2016

NREL is a national laboratory of the U.S. Department of Energy
Office of Energy Efficiency & Renewable Energy
Operated by the Alliance for Sustainable Energy, LLC

This report is available at no cost from the National Renewable Energy Laboratory (NREL) at www.nrel.gov/publications.

Conference Paper
NREL/CP-5J00-65682
June 2016

Contract No. DE-AC36-08GO28308

NOTICE

This report is available at no cost from the National Renewable Energy Laboratory (NREL) at www.nrel.gov/publications.

Available electronically at SciTech Connect http:/www.osti.gov/scitech

Available for a processing fee to U.S. Department of Energy and its contractors, in paper, from:

U.S. Department of Energy
Office of Scientific and Technical Information
P.O. Box 62
Oak Ridge, TN 37831-0062
OSTI http://www.osti.gov
Phone: 865.576.8401
Fax: 865.576.5728
Email: reports@osti.gov

Available for sale to the public, in paper, from:

U.S. Department of Commerce
National Technical Information Service
5301 Shawnee Road
Alexandria, VA 22312
NTIS http://www.ntis.gov
Phone: 800.553.6847 or 703.605.6000
Fax: 703.605.6900
Email: orders@ntis.gov

Cover Photos by Dennis Schroeder: (left to right) NREL 26173, NREL 18302, NREL 19758, NREL 29642, NREL 19795.

NREL prints on paper that contains recycled content.

Wild Band Edges: The Role of Bandgap Grading and Band-Edge Fluctuations in High-Efficiency Chalcogenide Devices

Ingrid Repins,[1] Lorelle Mansfield,[1] Ana Kanevce,[1] Søren A. Jensen,[1] Darius Kuciauskas,[1] Stephen Glynn,[1] Teresa Barnes,[1] Wyatt Metzger,[1] James Burst,[1] Chun-Sheng Jiang,[1] Patricia Dippo,[1] Steve Harvey,[1] Glenn Teeter,[1] C. Perkins,[1] Brian Egaas,[1] Andriy Zakutayev,[1] Jan-Hendrik Alsmeier,[2] Thomas Lußky,[2] Lars Korte,[2] Regan G. Wilks,[2] Marcus Bär,[2,3] Yanfa Yan,[4] Stephan Lany,[1] Pawel Zawadzki,[1,] Ji-Sang Park,[1] Suhuai Wei[1,5]

1. National Renewable Energy Laboratory, Golden, Colorado, 80401, U.S.A.
2. Solar Energy Research, Helmholtz-Zentrum Berlin für Materialien und Energie GmbH, 14109 Berlin, Germany
3. Institut für Physik und Chemie, Brandenburgische Technische Universität Cottbus-Senftenberg, 03044 Cottbus, Germany
4. Department of Physics and Astronomy, University of Toledo, Toledo, Ohio, 43606, U.S.A.
5. Beijing Computational Science Research Center, Beijing 100094, China

***Abstract* — Band-edge effects – including grading, electrostatic fluctuations, bandgap fluctuations, and band tails – affect chalcogenide device efficiency. These effects now require more careful consideration as efficiencies increase beyond 20%. Several aspects of the relationships between band-edge phenomena and device performance for NREL absorbers are examined. For Cu(In,Ga)Se_2 devices, recent increases in diffusion length imply changes to optimum bandgap profile. The origin, impact, and modification of electrostatic and bandgap fluctuations are also discussed. The application of the same principles to devices based on CdTe, kesterites, and emerging absorbers (Cu_2SnS_3, $CuSbS_2$), considering differences in materials properties and defect formation energies, is examined.**

***Index Terms* — CIGS, CdTe, CZTS, CTS, CAS, defect, grading, fluctuations.**

I. Introduction

Recent years have seen impressive increases in efficiencies for chalcogenide solar cells, allowing lower module and electricity costs. Improving device performance and semiconductor quality has prompted a re-examination of how spatial variations in the absorber band edges are understood and designed. Consideration of band-edge effects are relevant to all the chalcogenide absorbers made at NREL: $CuIn_xGa_{1-x}Se_2$ (CIGS), CdTe, $Cu_2ZnSnS_ySe_{4-y}$ (CZTSS), and new earth-abundant materials such as Cu_2SnS_3 (CTS) and $CuSbS_2$ (CAS). The sections below discuss how bandgap grading, band-edge fluctuations, and band-tailing are observed and affect device performance and design in different chalcogenide absorbers.

II. CIGS

A. Bandgap Grading

Intentional manipulation of band edges by alloying Ga with In, or S with Se, has been demonstrated and discussed thoroughly in the literature [1]-[8]. Bandgap profiles have been formed into "notch" structures, as illustrated by the composition profiles in Fig. 1. The solid lines indicate Ga/(In+Ga) atomic ratio extracted from Auger electron spectroscopy (AES), and dotted lines convert the Ga ratio to bandgap using previously derived formulae [9].

The left side of the notch is formed by a "front-grading" (from 0 to ~0.5 μm in Fig. 1), which reduces forward current, yet allows photocurrent to be largely controlled by the bandgap just beyond the front grading. Benefits and requirements for front grading have been discussed in the literature. [1],[7] Recent work has demonstrated performance benefit from use of a steeper front grading that better matches the device electric field in that region[7],[10]. In Fig. 1 this change is reflected by the deeper notch and steeper front grading in the orange curves compared to the older green curve.

The right side of the notch in Fig. 1, is formed by "back grading," a gradual bandgap increase from ~0.5 μm to the back of the film. Back grading has been identified as beneficial to for keeping minority carriers away from the high recombination velocity back interface, and for increasing carrier collection via the slope in the conduction band that separates photo-generated electron-hole pairs [1],[3].

However, recent changes to CIGS absorbers have increased diffusion lengths dramatically and require a re-thinking of the role of back grading. The evolution of diffusion length in CIGS devices is typified by the electron-beam induced current (EBIC) cross sections shown in Fig. 2. In the 1995 data, a clear decrease in signal is observed from left to right, indicative of a diffusion length smaller than the absorber thickness. In the 2012 data, carrier collection is flat with increased penetration into the absorber, indicating a much longer diffusion length. Minority carrier lifetime measurements on recent absorbers are consistent with this

observation. Minority carrier lifetimes are now routinely longer than 100 ns, and sometimes 200 to 400 ns [11],[12],[28]. A 200 ns lifetime implies an 8 μm diffusion length for 100 cm^2/V-sec mobility.

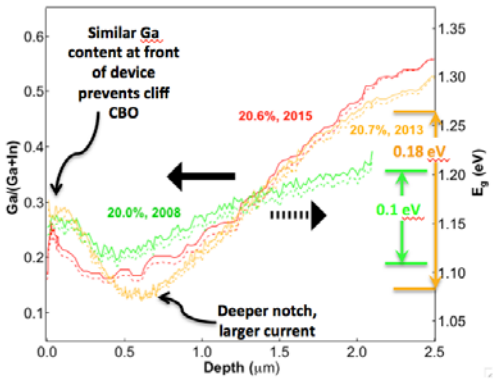

Fig. 1: Ga/(In+Ga) atomic ratio (left axis and solid lines) and band gap (right axis, dotted lines) for several NREL CIGS films.

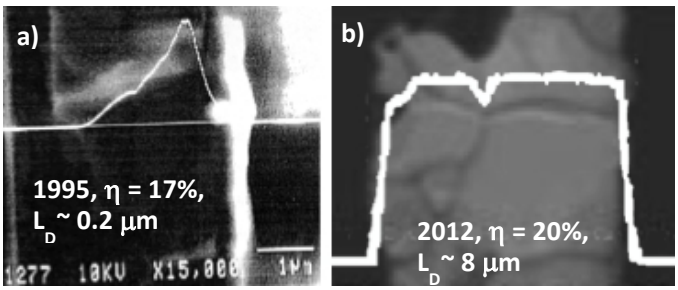

Fig. 2: EBIC cross-section images for NREL CIGS devices made in a) 1995 and b) 2012. For both images, the light incident side of the device is on the right. An x-y representation of one horizontal pass of the electron beam (e.g. a line scan) is superimposed on each intensity map.

Thus, the purported advantage of back-grading in increasing carrier collection is no longer valid in the modern CIGS device. While a back barrier is needed to reflect electrons away from the back contact, the carrier-collection function is not. In fact, the gradual nature of current back grading profiles causes photoabsorption loss. To illustrate this point, three hypothetical band gap gradings are shown in Fig. 3a. These band gap profiles were incorporated into a device model, with all band gap expansion occurring in the conduction band, consistent with Ga addition. Mid-gap defect concentration was set to yield a bulk lifetime of 50 ns, and other modeling input parameters were set as specified elsewhere [13],[14]. The resulting current-voltage (JV) and quantum efficiency curves output from the model are shown in Fig. 3b and c, with the JV parameters inset in Fig. 3b. The blue line in Fig. 3a shows a typical notch structure, whereas red line shows the same height of back barrier implemented as an abrupt step function. The gradual back grading profile operates at a higher voltage and lower photocurrent than the abrupt-barrier curve, since the gradual grading introduces a higher Ga content in and near the depletion region. However, a curve with gradual grading also suffers from incomplete red photocurrent absorption, as seen in Fig. 3c, resulting in a net lower efficiency. In fact, the parameters in Fig. 3c underreport the efficiency loss associated with the gradual grading, since this structure puts higher Ga contents near the depletion region, and - in reality - minority carrier lifetime decreases with increasing Ga content [12],[15].

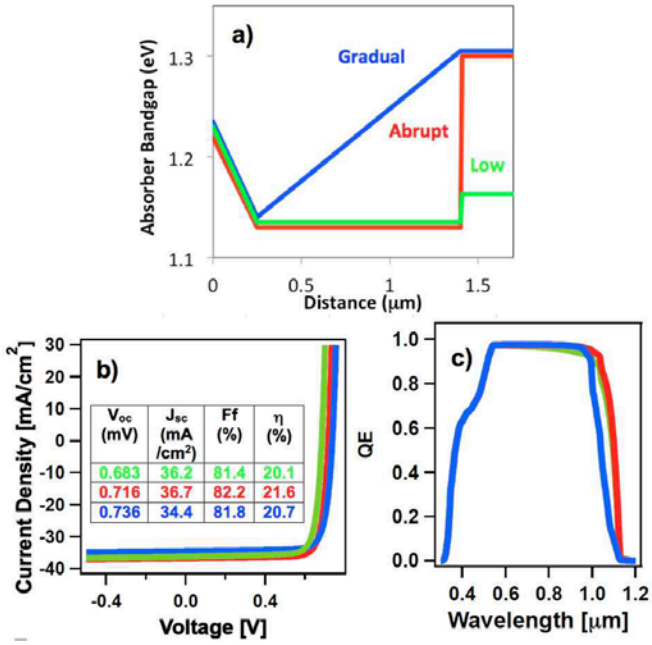

Fig. 3: a) Conduction band profiles showing typical notch structure (blue), abrupt back grading (red), and abrupt back grading with lower barrier (green); b) JV and c) QE curves resulting from utilizing above band gap profiles in modeled device.

The green line in Fig. 1 shows an abrupt grading, like the red profile, but with a lower barrier. Voltage from the green profile is lower because electrons can surmount the barrier and recombine at the back contact. Executing several models with barrier height between the red and green profiles indicate that for surface recombination velocities around 10^5 cm/sec, a back barrier in the range of 150 to 200 meV is needed for negligible voltage loss at the back contact. Recent changes in Ga profile at NREL (Fig. 1) and elsewhere[7],[10] reflect this need for a higher back contact barrier.

B. Band-Edge Fluctuations

Band edges in chalcopyrites exhibit unintentional variations from the abrupt and spatially-uniform character attributed to model systems. Such band-edge effects can be categorized into three types: i) bandgap variations, ii) electrostatic variations, where changes in free carrier concentration change the position of the band edges relative to the Fermi level, and iii) band tails, where localized states extend into the gap. Band-edge effects have been observed in CIGS by numerous techniques, for example micro-scale energy dispersive spectroscopy[16], cathodo-[17] or photo- luminescence [18]-[20], and capacitance techniques [21].

An example of spectral cathodoluminescence (CL) imaging indicating electrostatic fluctuations is shown in Fig. 4. Lower-energy emission is observed at the grain boundaries (GB) than in the grain interior (GI). The red shift in the luminescence at the grain boundary is attributed to band-bending there, as illustrated schematically in Fig. 5a, transition "1." Radiative transitions can occur at the band gap energy (labeled "3"), between shallow states (labeled "2"), or between neighboring areas of different electrostatic potential (lowest energy, labeled "1"). Variations with temperature and excitation intensity are also qualitatively consistent with band-edge fluctuations.[17]

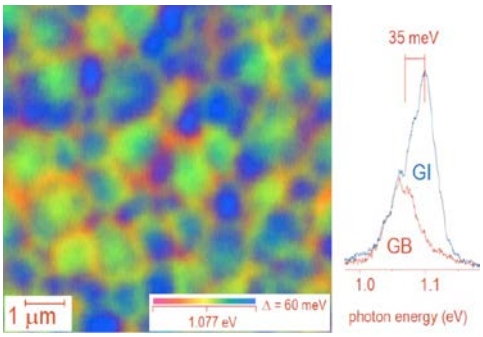

Fig. 4: Cathodoluminescence peak emission energy spatial map (left), and typical emission at grain boundary and grain interior (right). Measurement temperature is 19 K.

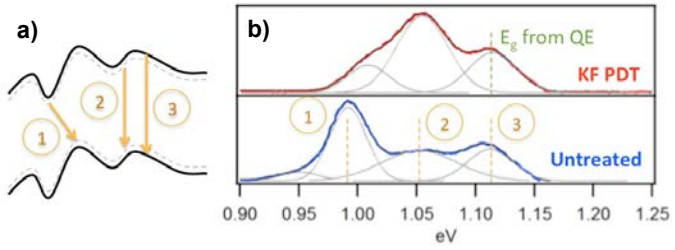

Fig. 5: a) Schematic representation of possible radiative transitions. b) 4.25K PL emission spectra from two CIGS samples made by the same recipe except with (top) or without (bottom) KF post-deposition treatment.

Some work has proposed that potential fluctuations at the grain boundary edge are necessary to serve as channels for carrier collection [22]. While this function may have been beneficial in older, shorter diffusion length CIGS, current high-efficiency absorbers do not need grain boundaries for carrier collection, as discussed related to Fig. 2. On the contrary, modeling [23],[24] and analytic studies [25],[26] have shown that band-edge fluctuations increase forward current are thus detrimental to device performance.

The three basic components shown in Fig. 5a are also observed in PL spectra. Fig. 5b shows low-temperature PL spectra, with components 1, 2, and 3 apparent. The use of a KF post-deposition treatment (PDT) [27] caused not only improvement in device voltage, but also a relative decrease in component 3 from potential fluctuations. Scanning kelvin probe force microscopy data on the same samples showed a reduction in band-bending at the grain boundaries with application of the KF PDT [28]. Thus, the KF PDT serves as an example of a processing change that manipulates band-edge fluctuations (among other effects).

III. CdTe

Polycrystalline CdTe properties have undergone a transformation in recent years that is perhaps even more dramatic than that in CIGS. For example, Fig. 6 uses published data [29]-[33] to illustrate the trend toward long lifetimes and consequently higher device voltage.

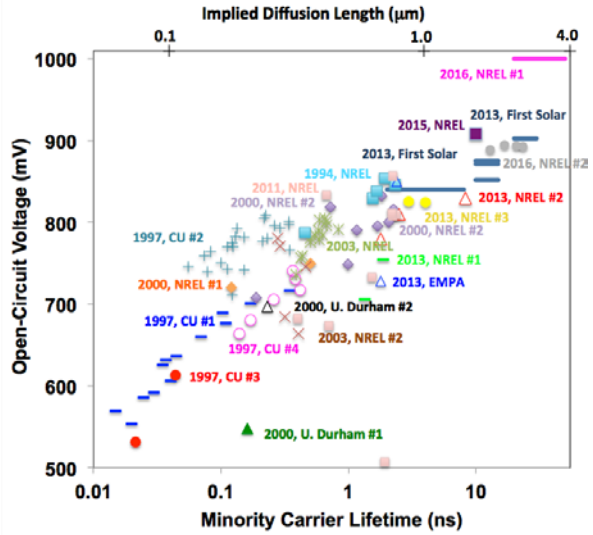

Fig. 6. Published lifetime and voltage data for CdTe devices spanning ~20 years. On the top axis, lifetime is converted to diffusion length by assuming a hole mobility of 100 cm^2/V-sec.

For the highest quality devices, diffusion length is approaching film thickness. Thus, in the future, electron reflection may be helpful for CdTe devices as discussed earlier for long-diffusion-length CIGS. To date, ohmicity and stability have been the predominant goals in making CdTe back contacts, which are challenging due to the material's large electron affinity. Based on band alignment, ZnTe [34] may provide a suitable electron reflector, but has not been studied widely. Traditionally, CdTe devices have not implemented designed bandgap grading and there is an opportunity for more aggressive alloying efforts to increase efficiency in a parallel path to that of CIGS. For example, quantum efficiency data on recent record devices [35] shows response at photon energies down to 1.40 eV, well below the 1.5 eV CdTe bandgap.

In CdTe, potential fluctuations are observed at the grain boundaries due to intentionally-introduced extrinsic impurities such as Cl [36],[37]. While grain-boundary passivation is important, a collection path at grain boundaries is not needed and electrostatic fluctuations there increase forward current., analogous to the case of CIGS. Passivating grain boundaries without inducing electrostatic fluctuations can be helpful.

Alternate strategies are to reduce grain-boundary recombination without significant band-bending, or to repel carriers by introducing a larger bandgap material there.

IV. CZTS

An understanding of the relative occurrence of band-edge effects in CdTe, CIGS, and CZTS can be gained from an examination of the calculated defect formation energies. Fig. 7 shows defect formation energies as a function of Fermi energy as compiled from published density functional theory calculations [38],[39],[40].

Fig. 7a shows defect formation energies for Te-rich CdTe. The lowest formation energy defect is the anion vacancy, V_{Te}, a shallow donor that can limit free hole density. For the Fermi level position resulting from modest free hole densities thus achieved in near-equilibrium CdTe, other defect formation energies are over 1 eV. This relatively high formation energy for most intrinsic defects is consistent observation of band edge fluctuations in CdTe mostly from *extrinsic* defects (e.g. Cl at grain boundaries). In contrast, for Cu-poor CIGS, Fig. 7b, both the copper vacancy (V_{Cu}) and clusters of V_{Cu} with the In on Cu antisite (In_{Cu}) have formation energies of less than 0.5 eV. Thus, the observation of band-edge effects related to Cu variations [16] is not surprising.

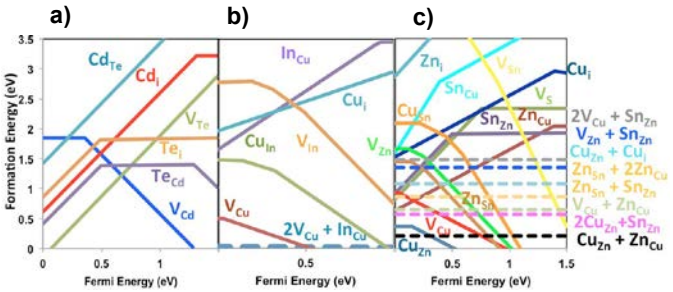

Fig. 7: Defect formation energies for a) Te-rich CdTe, b) Cu-poor CIGS, and c) Cu-poor CZTS.

Comparing formation energies of Cu-poor CZTS (Fig. 7c) to those in CIGS or CdTe, it is apparent that a much wider array of intrinsic defects and defect clusters with low formation energy exist. Thus, it should be expected that CZTS exhibits a larger tendency toward disorder, band tails, and band-edge fluctuations. A number of studies have observed such effects (for example, [20],[41],[42]). A comparison of NREL CIGS and $Cu_2ZnSnSe_4$ (CZTSe) by constant final state yield spectroscopy indicates that the concentration of near-band-edge states is three to five times higher for CZTSe than for CIGS [46]. Furthermore, CZTSe exhibits a higher Urbach energy than CIGS in these tests, indicating that the near-band-edge states penetrate deeper into the gap. An order-disorder transition temperature has been predicted from first principles [43], and observed experimentally [44],[45]. At NREL, successive anneals were performed on devices in the sequence shown in Fig. 8, to induce the ordered or disordered state, as PL emission spectra were measured in-situ. When anneals were performed at 200 C or above, PL emission was ~100 meV lower than after anneals performed below the transition temperature.

After each anneal, a JV measurement was performed. Surprisingly, open-circuit voltage (V_{oc}) did not follow the PL peak emission strongly, as one would expect if an abrupt change in band gap were occurring. For the device of Fig. 8, V_{oc} was unchanged after each anneal. The behavior of several devices was explored in this manner, and a maximum V_{oc} increase of 30 mV was observed. In no case did the V_{oc} change approach the 100 mV that might be expected from the PL shift. Furthermore, the disordered state always yielded a slightly higher performance, since any small increase in V_{oc} was accompanied by a decrease in short-circuit current.

The anneals of Fig. 8 and those described in the literature [44],[45] clearly affect disorder in the sample and the band edges. However, theses studies have not yet demonstrated substantial V_{oc} increase. It must be concluded that either 1) the anneals do not remove enough states near the band-edges to markedly decrease recombination, or 2) a property unaffected by these anneals (possibly a different set of intrinsic defects) controls the performance.

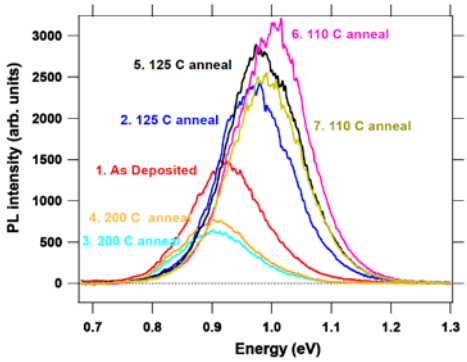

Fig. 8: Room temperature PL emission spectra of completed CZTSe device after an anneal at the labeled temperature. The numeral at the beginning of each label shows the order in which the successive anneals were performed.

V. Emerging Absorbers

Another important research direction is to find emerging absorbers that would not be as prone to detrimental band edge effects. Since the number of possible intrinsic defects increases with increasing number of elements, one possibility is to look for materials that are more chemically simple than quaternary CZTS but have similar tetrahedrally-bonded diamond-derived crystal structure, such as ternary CTS or CAS. Another option is to keep the chemical complexity the same (e.g. ternary material) and change the crystal structure from 3D-like to lower dimensions, such as 2D-like CAS or 1D-like Sb_2S_3, where the element coordinations may be sufficiently different to prevent disorder.

To expand on the first option, recent NREL theoretical calculations using model Hamiltonian and Monte Carlo

simulations, [43] indicate that cation disorder in CTS leads to entropy-driven cation clustering. The atomistic mechanism for these imperfections in CTS is different than that in CZTS, but the end result is the same: nanoscale compositional inhomogeneities can cause potential fluctuations. The follow-up experiments confirm that more cation order in CTS can be induced by prolonged annealing, but the resulting samples still have very short ps-scale lifetimes [47]. Another related theoretically-predicted phenomenon is the formation of extended antisite defects that involve complex, nonlocal atomic rearrangements that cannot be captured within a simple point defect model [48]. These effects can lower the formation energy and lead to large deviations from stoichiometry. Indeed, combinatorial experiments indicate that hole concentration in CTS can be tuned over 3 orders of magnitude by increasing its Cu content almost up to Cu_3SnS_4 composition, without any CuS_x precipitation [49]. Thus, it appears that making materials chemically simpler can help solve some of the band-edge related problems, but can also lead to other unintended consequences.

The second possibility - changing the crystal structure from 3D-like to lower dimension - is scientifically exciting but also quite challenging. For example $CuSbQ_2$ (Q=S,Se) has the same 1:1:2 stoichiometry and $Cu(In,Ga)Q_2$, plus similar band gaps and hole doping levels. However, compared to the chalcopyrite, the layered chalcostibite crystal structure of $CuSbQ_2$ (CAS) leads to a larger density of states and hence higher optical absorption but larger effective masses. In addition, even small deviations from Cu:Sb=1:1 stoichiometry should lead to phase impurities, in sharp contrast with CIGS, CTZS and CTS where as high as 20% off-stoichiometry is possible. These points come from the recent experimental and theoretical work [50]-[52] at NREL. Another challenge related to CAS chalcostibite PV devices is replacing the usual CdS buffer layer with an alternative heterojunction partner that has higher conduction band position. 1D-like materials such as Sb_2Q_3 [53] are also potentially promising.

VI. Conclusions

The roles of band-edge effects in chalcogenide device performance can be summarized as follows: Bandgap front- and back- grading can enhance device performance. In long diffusion length absorbers, back grading is useful only for electron reflection, not carrier collection. A gradual back grading causes incomplete red collection: an abrupt electron reflector is preferable. Potential fluctuations at the grain boundaries are no longer needed for carrier collection, due to improved diffusion lengths in CIGS and CdTe. Rather, these potential fluctuations increase forward current and decrease voltage. Types of band-edge fluctuations are observed in all chalcogenide absorbers made at NREL, and are consistent with expectations from the defect formation energies. In CdTe, extrinsic defects cause electrostatic fluctuations at the grain boundaries. While such fluctuations currently minimize the effect of high recombination velocity at the grain boundary, they may also ultimately limit performance. Grain boundary defect passivation, or bandgap expansion there, are potentially higher-performance alternatives. In CIGS, there is evidence for electrostatic and bandgap fluctuations, both within the grain and at the grain boundaries. Recent advances in CIGS device performance at NREL utilize changes in the bandgap grading and manipulation of potential fluctuations via PDT. For CZTS, calculations indicate numerous intrinsic defects and defect clusters with low formation energies. Thus, it should be expected that CZTS exhibits a larger tendency toward disorder, band tails, and band-edge fluctuations, as observed experimentally. Less chemically complex materials (e.g. CTS) and non-diamond crystal structures (e.g. CAS) may reduce detrimental band edge effects, but also pose other challenges for efficient PV device engineering. As efficiencies of the best CdTe and CIGS devices continue to increase well beyond 20%, the necessity of controlling band-edge effects to reach and surpass these levels of performance sets a very high bar for new materials.

Acknowledgements

The authors gratefully acknowledge the lasting contribution of Dr. Manuel Romero to the subject of band-edge fluctuations. This research was supported by the U.S. Department of Energy, Energy Efficiency and Renewable Energy, under Contract No. DE-AC36-08GO28308. The U.S. Government retains and the publisher, by accepting the article for publication, acknowledges that the U.S. Government retains a nonexclusive, paid up, irrevocable, worldwide license to publish or reproduce the published form of this work, or allow others to do so, for U.S. Government purposes.

References

[1] M. Gloeckler, and J.R. Sites, "Band-gap grading in $Cu(In,Ga)Se_2$ solar cells," *J. of Phys. Chem. Solids*, vol. 66, pp. 1891-1894, 2005.

[2] A.M. Gabor *et al.*, "Band-gap engineering in $Cu(In,Ga)Se_2$ thin films grown from $(In,Ga)_2Se_3$ precursors," *Sol. Energ. Mat. Sol. C.*, vol. 41-42, pp. 247-260, 1996.

[3] T. Dullweber *et al.*, "Back surface band gap gradings in $Cu(In,Ga)Se_2$ solar cells," *Thin Solid Films,* vol. 387, pp. 11–13, 2001.

[4] S. Schleussner, U. Zimmermann, T. Wätjen, K. Leifer, and M. Edoff, "Effect of gallium grading in $Cu(In,Ga)Se_2$ solar-cell absorbers produced by multi-stage coevaporation," *Sol. Energ. Mat. Sol. C.*, vol. 95, pp. 721–726, 2011.

[5] S.H. Song *et al.*, "Structure optimization for a high efficiency CIGS solar cell," in *Proc. IEEE 35th Photovoltaic Spec. Conf.,* 2010, pp. 2488-2492.

[6] T.M. Friedlmeier *et al.*, "Improved Photocurrent in $Cu(In,Ga)Se_2$ Solar Cells: From 20.8% to 21.7% Efficiency with CdS Buffer and 21.0% Cd-Free," *IEEE J. Photovoltaics*, Vol. 5, pp. 1487-1491, 2015.

[7] A. Chirila *et al.*, "Highly efficient $Cu(In,Ga)Se_2$ solar cells grown on flexible polymer films," *Nat. Mater.*, vol.10, pp. 857-861, 2011.

[8] W. Witte *et al.*, "Gallium gradients in Cu(In,Ga)Se2 thin-film solar cells" *Prog. Photovoltaics,* vol. 23, pp. 717–733, 2015.

[9] A. Rocket, "Performance-limitations in Cu(In,Ga)Se2-based heterojunction solar cells," in *Proc. IEEE 29th Photovoltaic Spec. Conf.,* 2002, pp. 587–591.

[10] P. Jackson *et al.*, "Properties of Cu(In,Ga)Se2 solar cells with new record efficiencies up to 21.7%," *Phys. Status Solidi RRL*, vol. 9, pp. 28–31, 2015.

[11] W.K. Metzger, I.L. Repins, and M.A. Contreras, "Long lifetimes in high-efficiency $Cu(In,Ga)Se_2$ solar cells," *Appl. Phy. Lett.*, vol. 93, art. no. 022110, 2008.

[12] J.V. Li *et al.*, "A recombination analysis of $Cu(In,Ga)Se_2$ solar cells with low and high Ga compositions," *Sol. Energ. Mat. Sol. C.*, vol. 124, pp. 143–149, 2014.

[13] A. Kanevce, K. Ramanathan, M. Contreras, "Impact of buffer and absorber properties in the vicinity of the interface on wide-gap Cu(In,Ga)Se2 solar cell performance," in *Proc. IEEE 40th Photovoltaic Spec. Conf.*, 2014, pp. 382-386.

[14] M. Gloeckler, A.L. Fahrenbruch, and J.R. Sites, "Numerical modeling of CIGS and CdTe solar cells: setting the baseline," in *Proc. 3rd World Conf. Photovoltaic Energ. Conv.*, 2003, pp. 491–494.

[15] B. Huang *et al.*, "Origin of Reduced Efficiency in $Cu(In,Ga)Se_2$ Solar Cells With High Ga Concentration: Alloy Solubility Versus Intrinsic Defects, *IEEE J. Photovoltaics*, vol. 4, pp. 477-482, 2014.

[16] Y. Yan *et al.*, "Chemical fluctuation-induced nanodomains in $Cu(In, Ga)Se_2$ films," *Appl. Phy. Lett.,* vol. 87, art. no. 121904, 2005.

[17] M.J. Romero *et al.*, "Cathodoluminescence of $Cu(In,Ga)Se_2$ thin films used in high-efficiency solar cells," *Appl. Phy. Lett.*, vol. 83, art. no. 4770, 2003.

[18] L. Gütay, C. Lienau, and G. H. Bauer, "Subgrain size inhomogeneities in the luminescence spectra of thin film chalcopyrites," *Appl. Phy. Lett.*, vol. 97, art. no. 052110, 2010.

[19] Y.-K. Liao *et al.*, "Observation of unusual optical transitions in thin-film $Cu(In,Ga)Se_2$ solar cells," *Opt. Express*, vol. 20, pp. A836-A842, 2012.

[20] M. Okano, L.Q. Phuong, and Y. Kanemitsu, "Photocarrier dynamics in CIGS, CZTS, and related materials revealed by ultrafast optical spectroscopy," *Phys. Status Solidi B*, vol. 252, pp. 1219–1224, 2015.

[21] J.T. Heath, J. D. Cohen, W. N. Shafarman, D. X. Liao, and A. A. Rockett, "Effect of Ga content on defect states in $CuIn_{1-x}Ga_xSe$ photovoltaic devices," *Appl. Phy. Lett.*, vol. 80, pp. 4540-4542, 2002.

[22] J.B. Li, V. Chawla, and B.M. Clemens, "Investigating the Role of Grain Boundaries in CZTS and CZTSSe Thin Film Solar Cells with Scanning Probe Microscopy," *Adv. Mater*., vol. 24 pp. 720–723, 2012.

[23] W. K. Metzger and M. Gloeckler, "The impact of charged grain boundaries on thin-film solar cells and characterization," *J. Appl. Phys.*, vol. 98, art. no. 063701, 2005.

[24] A. Kanevce, I. Repins, and S.-H. Wei, "Impact of bulk properties and local secondary phases on the $Cu_2(Zn,Sn)Se_4$ solar cells open-circuit voltage," *Sol. Energ. Mat. Sol. C.,* vol. 133, pp. 119–125, 2015.

[25] J.H. Werner, J. Mattheis, and U. Rau, "Efficiency limitations of polycrystalline thin film solar cells: case of $Cu(In,Ga)Se_2$," *Thin Solid Films*, vol. 480–481, pp. 399– 409, 2005.

[26] S. Siebentritt, "What limits the efficiency of chalcopyrite solar cells?" *Sol. Energ. Mat. Sol. C.,* vol. 95, pp. 1471–1476, 2011.

[27] A. Chirila *et al.*, "Potassium-induced surface modification of $Cu(In,Ga)Se_2$ thin films for high-efficiency solar cells," *Nat. Mater.*, vol. 12, pp. 1107-1111, 2013.

[28] S.A. Jensen *et al.*, "Beneficial effect of post-deposition treatment in high-efficiency $Cu(In,Ga)Se_2$ solar cells through reduced potential fluctuations," under review at *J. Appl. Phys.*.

[29] J.M. Burst *et al.*, "CdTe solar cells with open-circuit voltage breaking the 1V barrier," *Nat. Energ.*, vol. 1, art. no. 16015, 2016.

[30] J.N. Duenow *et al.*, "Single-crystal CdTe solar cells with V_{oc} greater than 900mV," *Appl. Phy. Lett.*, vol. 105, art. no. 053903, 2014.

[31] W. Metzger *et al.*, "Time-resolved photoluminescence studies of CdTe solar cells," *J. Appl. Phys.*, vol. 94, pp. 3549-3555, 2003.

[32] D. Kuciauskas *et al.*, "Recombination Analysis in Cadmium Telluride Photovoltaic Solar Cells With Photoluminescence Spectroscopy," *IEEE J. Photovoltaics*, vol. 6, pp. 313-318, 2016.

[33] M. Gloeckler, I. Sankin, and Z. Zhao, "CdTe Solar Cells at the Threshold to 20% Efficiency," *IEEE J. Photovoltaics*, vol. 3, pp.1389-1393, 2013.

[34] M. Gloeckler, L. Cheng, "Method and apparatus for forming a cadmium telluride layer in a photovoltaic device," U.S. patent application #20140374266, 12/25/2014.

[35] M.A. Green, K. Emery, Y. Hishikawa, W. Warta, and E.D. Dunlop, "Solar cell efficiency tables (version 46)," *Prog. Photovoltaics,* vol. 23, pp. 805–812, 2015.

[36] S.P. Harvey, G. Teeter, H. Moutinho, and M.M. Al-Jassim, "Direct evidence of enhanced chlorine segregation at grain boundaries in polycrystalline CdTe thin films via three-dimensional TOF-SIMS imaging," *Prog. Photovoltaics,* vol 23, pp. 838–846, 2014.

[37] C.-S. Jiang, H.R. Moutinho, J. Duenow, E. Colegrove, W. Metzger, and M.M. Al-Jassim, in preparation.

[38] S.-H. Wei and S.B. Zhang, "Chemical trends of defect formation and doping limit in II-VI semiconductors: The case of CdTe," *Phys. Rev. B*, vol. 66, art. no. 155211, 2002.

[39] J.-H. Yang *et al.*, "Tuning the Fermi level beyond the equilibrium doping limit through quenching: The case of CdTe," *Phys. Rev. B*, vol. 90, art. no. 245202, 2014.

[40] S. Chen, A. Walsh, X.-G. Gong, and S.-H. Wei, "Classification of Lattice Defects in the Kesterite Cu_2ZnSnS_4 and $Cu_2ZnSnSe_4$ Earth-Abundant Solar Cell Absorbers," *Adv. Mat.,* vol. 25, pp. 1522-1539, 2013.

[41] T. Gokmen, O. Gunawan, T.K. Todorov, and D.B. Mitzi, "Band tailing and efficiency limitation in kesterite solar cells," *Appl. Phy. Lett.*, vol. 103, art. no. 103506, 2013.

[42] L. Van Puyvelde *et al.*, "Photoluminescence investigation of Cu_2ZnSnS_4 thin film solar cells," *Thin Solid Films,* vol. 582, pp. 146–150, 2015.

[43] P. Zawadzki, A. Zakutayev, and S. Lany, "Entropy-Driven Clustering in Tetrahedrally Bonded Multinary Materials," *Phys. Rev. Appl.*, vol. 3, art. no. 034007, 2015.

[44] J. S. Scragg, L. Choubrac, A. Lafond, T. Ericson, and C. Platzer-Björkman, "A low-temperature order-disorder transition in Cu_2ZnSnS_4 thin films," *Appl. Phy. Lett.*, vol. 104, art. no. 041911, 2014.

[45] G. Rey *et al.*, "The band gap of $Cu_2ZnSnSe_4$: Effect of order-disorder," *Appl. Phys. Lett.*, vol. 105, art. no. 112106, 2014.

[46] J.-H. Alsmeier, T. Lußky, L. Korte, R.G. Wilks, M. Bär, in progress.

[47] L.L. Baranowski *et al.*, "Effects of Disorder on Carrier Transport in Cu_2SnS_3," *Phys. Rev. Appl.,* vol. 4, art. no. 044017, 2015.

[48] P. Zawadzki, A. Zakutayev, and S. Lany, "Extended antisite defects in tetrahedrally bonded semiconductors," *Phys. Rev. B*, vol. 92, art. no. 201204(R), 2015.

[49] L.L. Baranowski *et al.,* "Control of doping in Cu_2SnS_3 through defects and alloying," *Chem. Mater.*, vol. 26, pp. 4951-4959, 2014.
[50] A.W. Welch, P.P. Zawadzki, S. Lany, C.A. Wolden, and A. Zakutayev, "Self-regulated growth and tunable properties of $CuSbS_2$ solar absorbers," *Sol. Energ. Mat. Sol. C.,* vol. 132, pp. 499-506, 2014.
[51] A.W. Welch *et al.*, "Accelerated development of $CuSbS_2$ thin film photovoltaic device prototypes," *Prog. Photovoltaics*, in press, 2016.
[52] A.W. Welch *et al.*, "$CuSbSe_2$ photovoltaic devices with 3% efficiency," *Appl. Phys. Exp*., vol. 8, art. no. 082301, 2015.
[53] Y. Zhou *et al.*, "Thin-film Sb_2Se_3 photovoltaics with oriented one-dimensional ribbons and benign grain boundaries," *Nat. Photonics*, vol. 9, pp.409-415, 2015.